ARTICLE

Flexible Germanium Nanowires: Ideal Strength, Room Temperature Plasticity, and Bendable Semiconductor Fabric

Damon A. Smith, Vincent C. Holmberg, and Brian A. Korgel*

Department of Chemical Engineering, Texas Materials Institute, and Center for Nano- and Molecular Science and Technology, The University of Texas at Austin; Austin, Texas 78712-1062

ABSTRACT The mechanical strengths of individual germanium (Ge) nanowires with ⟨111⟩ growth direction and diameters ranging from 23 to 97 nm were measured by bending each with a robotic nanomanipulator in a scanning electron microscope (SEM). The nanowires tolerate diameter-dependent flexural strains of up to 17% prior to fracture, which is more than 2 orders of magnitude higher than bulk Ge. The corresponding bending strength of 18 GPa is in agreement with the ideal strength of 14−20 GPa for a perfect Ge crystal. Nanowires also exhibited plastic deformation at room temperature, becoming amorphous at the point of maximum strain. A bendable, nonwoven fabric, or paper, of Ge nanowires is demonstrated.

KEYWORDS: nanowires · mechanical properties · germanium · nanomanipulation · nanomechanics

Germanium (Ge) is a brittle material.[1] Only at high temperature, greater than 350 °C, does it exhibit any measurable ductility.[2] This is because plastic deformation requires the nucleation and movement of dislocations, which is largely blocked by the directional, covalent bonding between germanium (Ge) atoms (the Peierls force). Therefore, unless the temperature is very high, a bulk crystal of Ge fractures when deformed just past its yield point.[3] Ge crystals also tend to be relatively fragile because they have nearly unavoidable defects and stresses that serve as sources for crack formation and propagation. Typical room temperature fracture strengths are only between 40 to 95 MPa, which is orders of magnitude less than the ideal strength expected for a perfect Ge crystal of 14−20 GPa.[4,5] Nanowires are different. Their limited size and high surface area to volume ratio leads to reduced concentrations of defects and stresses, and fracture strengths nearing those of ideal perfect crystals have been observed.[2,6−11] Nanowires do not sustain dislocations in the same way as bulk crystals, and plastic deformation mechanisms are different. For example, plastic deformation has even been observed in Si nanowires at room temperature.[12,13]

Herein, we show that Ge nanowires exhibit room temperature plasticity under certain bending conditions, enabled by an unusual mechanism of lattice amorphization.[14] The Ge nanowires were also found to exhibit ideal strengths. They represent a mechanically flexible, semiconductor material. We also demonstrate that the ability to make significant quantities of nanowires provides the opportunity to create a new class of materials: bendable fabrics of crystalline inorganic semiconductors.

Table 1 shows a list of selected materials and their room temperature mechanical properties of elastic modulus, tensile strength, failure strain, and strength-to-weight ratio. There has been a tremendous amount of attention on single- and multiwall carbon nanotubes as new structural reinforcements because of their incredibly high strength-to-weight ratio. Semiconductor nanowires, like Ge, should also exhibit very high strength-to-weight ratios-on par with Kevlar. Furthermore, nanowires can be dispersed relatively easily in various solvents by coating their surfaces with ligands.[9] Nonetheless, these materials have received much less attention for structural applications, primarily because of the need for synthetic methods to make them in large quantities.

We have developed a solvent-based approach to VLS-like growth of semiconductor nanowires, called supercritical fluid−liquid−solid (SFLS) growth, which enables the production of large amounts of nanowires.[7,8] For example, more than 1 g of Ge nanowires can be produced in a single reaction in a 250 mL vessel. This approach

*Address correspondence to korgel@che.utexas.edu.

Received for review February 15, 2010 and accepted March 18, 2010.

Published online March 31, 2010. 10.1021/nn1003088

TABLE 1. Mechanical Properties (Measured) of Selected Fibers, Nanotubes, and Nanowires

material	elastic modulus (GPa)	tensile strength (GPa)	failure strain (%)	strength-to-weight ratio (kN · m/kg)
Kevlar 49[a]	125	3.5	2.3	24.3
Nomex[a]	10	0.5	22	3.6
E-glass[a]	75	3.5	4	13.6
aluminum oxide[a]	350−380	1.7		4.6
carbon fiber T-300[a]	235	3.2	1.4	18.2
carbon fiber M60J[a]	585	3.8	0.7	19.6
stainless steel (18−8)[a]	198	1.0−1.4		1.8
tungsten[a]	360	5.5		0.28
SWCNT/MWCNT[b]	~1000	11−63	5−12	85−485
Si nanowire[c]	187	12	7	51.5
Ge nanowire	106[d]	18[e]	17[e]	33.8[e]

[a]From reference 11. [b]From reference 15. [c]From reference 16. [d]From reference 17. [e]This study.

provides enough material to explore new applications of semiconductor nanowires, like fibers and fabrics. Nanowires of materials that are typically brittle, are flexible and strong, and can exhibit a distinctive combination of electronic, optical, and mechanical properties, important for a variety of new device technologies, including next generation flexible electronics, nanoelectromechanical systems (NEMS), piezoelectronics, and structural materials.[16,18−22]

Many mechanical property measurements of individual nanowires exist in the literature,[20,23] but there is still a need for accurate quantitative data, especially considering that different synthetic routes can produce nanowires (of the same material) with varying properties depending on subtle aspects of the materials, like crystallographic growth direction, defects, and surface chemistry. We were particularly interested in the mechanical properties of SFLS-grown Ge nanowires under significant mechanical load. Commonly used mechanical tests, like bend tests in an atomic force microscope (AFM)[10,20,24,25] and tests of nanowire cantilevers under electric field-induced resonance,[16,26] work well for ex-

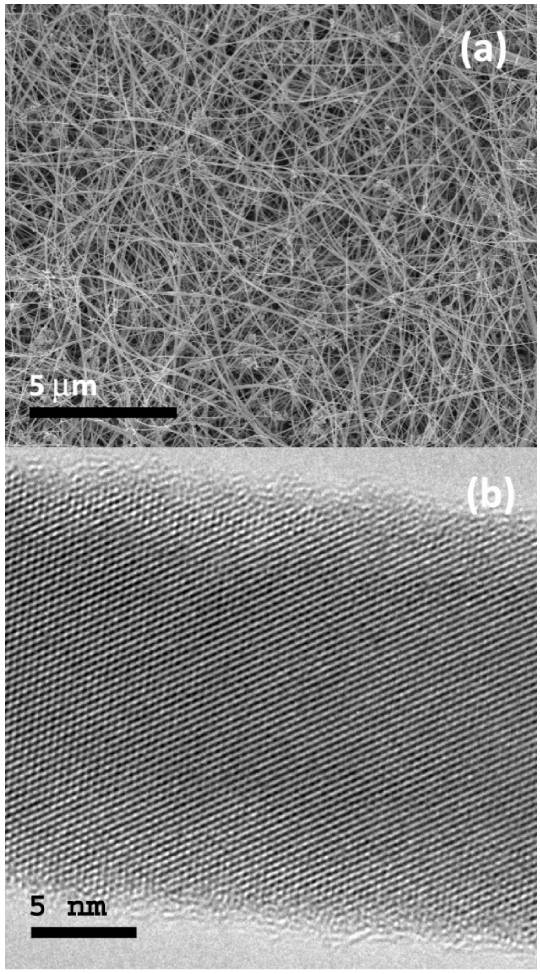

Figure 1. (a) SEM and (b) HRTEM images of Ge nanowires used for the mechanical property tests.

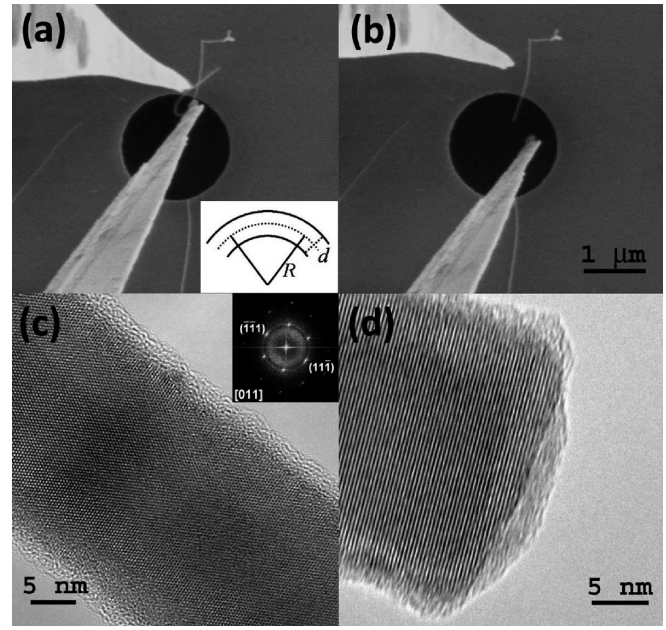

Figure 2. (a,b) SEM and (c,d) TEM images of a manipulated Ge nanowire. In panels a and b, the nanowire is being manipulated with two tungsten nanomanipulator probes. The bent nanowire in panel a is shown in panel b after it has fractured. Inset: Schematic of a bent nanowire. TEM images of the fractured Ge nanowire were acquired (c) near the substrate (inset: FFT of image) and (d) at the fractured surface.

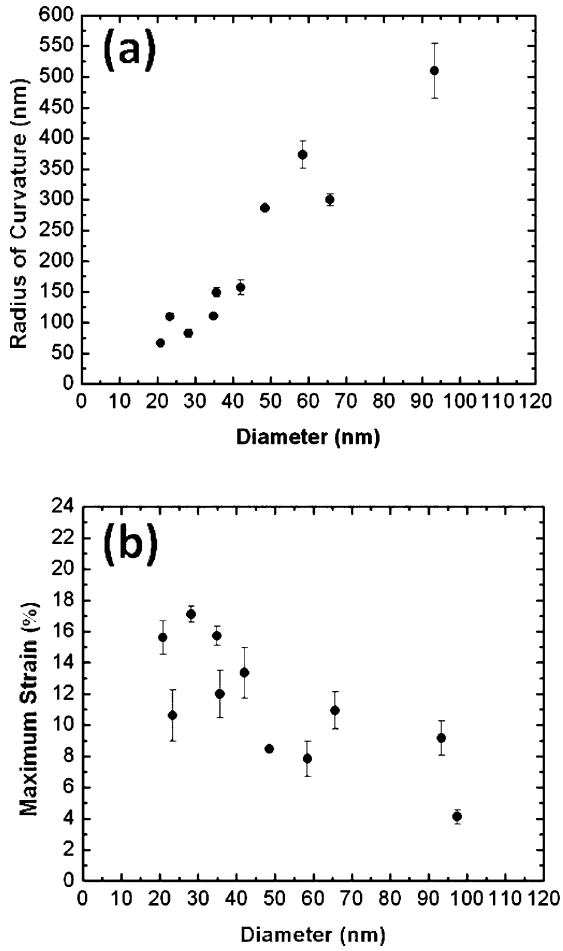

Figure 3. Maximum (a) radius of curvature and (b) flexural strain measured for Ge nanowires of varying diameter. All nanowires had ⟨111⟩ growth directions, as determined from FFTs of HRTEM images (Figure 2c inset).

amining the elastic properties of the nanowires, but are difficult to use for determining properties like the limit of flexibility and bending strength. Therefore, we used robotic nanomanipulation in an SEM to test individual nanowires under high flexural strain with simultaneous imaging to determine the maximum strain and fracture strengths of the nanowires.

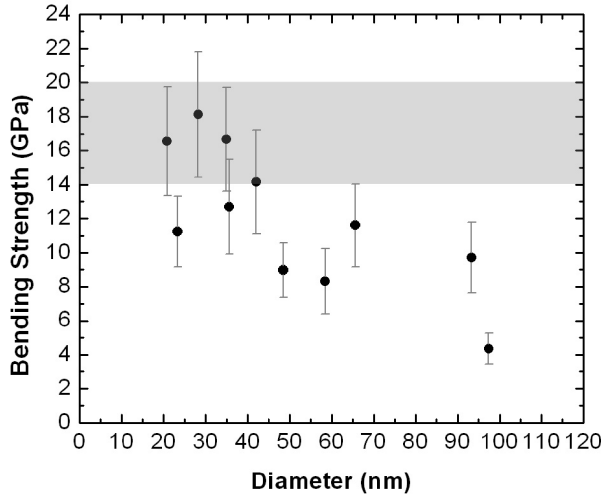

Figure 4. Bending strength measured for Ge nanowires of varying diameter. The gray shaded region corresponds to the predicted fracture strength for a perfect Ge crystal.[4,5]

RESULTS AND DISCUSSION

Figure 1 shows TEM and SEM images of the nanowires used in the study: nanowire diameters ranged from 23 to 97 nm, with crystalline diamond cubic Ge cores. For mechanical testing, Ge nanowires were drop-cast from a chloroform dispersion onto TEM grids coated with a silicon nitride membrane arrayed with 2 μm diameter holes (DuraSiN). An individual nanowire spanning a hole in the membrane was then located in the SEM. A nanomanipulator probe was then used to break the suspended nanowire on one end, close to the membrane. Using two tungsten probes, the nanowire was then bent parallel to the focal plane to determine the bending radius. Figure 2 shows an example of a typical manipulation of a Ge nanowire and the Supporting Information contains movies of individual nanowires being bent in this system.

The flexural strain of the nanowires was determined from the radius of curvature R, resolved from captured video images. The strain ε_x, at a distance x from the neutral axis is related to R as $\varepsilon_x = x/R$, and the maximum flexural strain at the point of fracture $\varepsilon_{\max,T}$ occurs at the nanowire surface on the outside of the bend (illustrated in the inset in Figure 2a). $\varepsilon_{\max,T}$, therefore, relates to the nanowire diameter d and the radius of curvature R:

$$\varepsilon_{\max,T} = \frac{d}{2R} \tag{1}$$

The stress σ_x in the nanowire at a distance x from the neutral axis is proportional to the strain, $\sigma_x = E\varepsilon_x$, where E is the Young's modulus. Bending leads to simultaneous tensile and compressive stresses; however, for Ge, the compressive strength is expected to be an order of magnitude larger than the tensile strength,[27] and the surface undergoing tensile strain is the expected point of failure. Therefore, the maximum tensile stress at fracture corresponds to the bending strength σ_{bs}, approximated by

$$\sigma_{bs} = E\varepsilon_{\max,T} = E\frac{d}{2R} \tag{2}$$

The maximum radius of curvature and flexural strain prior to fracture was measured for nanowires with ⟨111⟩ growth direction with diameters ranging from 23 to 97 nm. The measurements were conducted at strain rates typical for quasi-static strength tests of approximately 10^{-3} s^{-1}. Figure 3 shows the maximum radius of curvature and corresponding flexural strain for the nanowires. The flexural strain increased systematically with decreasing nanowire diameter from 4% to 17%, and the maximum strain

observed in the nanowires was much greater than the 0.04−0.06% measured for bulk Ge.[5]

The trend of increasing bending strength with decreasing diameter is clear. Taking $E = 106 \pm 19$ GPa, as previously measured for SFLS-grown Ge nanowires,[16] bending strengths estimated using eq 2 ranged from 4 ± 1 GPa for the largest diameter nanowire to up to 18 ± 4 GPa for the smallest diameters. The bending strengths of the nanowires in this size range fall in the range of the approximate maximum strength of a perfect crystalline solid of $E/2\pi$ (shaded region in Figure 4),[4] and the ideal strength of 14 GPa (tensile load) predicted by Roundy and Cohen[28] for a perfect Ge crystal. The bending strength is 2−3 orders of magnitude greater than bulk Ge. Similar results of size-dependent fracture strengths have also been observed for Si nanowires.[29−31] The increase in flexibility and strength with decreased diameter follows from the absence of extended defects in these crystals.[2]

Ge nanowires bent to a position of very high strain and released prior to fracture were found to exhibit plastic deformation (Figure 5, see Supporting Information for movie). When a nanowire was released, it snapped back quickly, but retained some of its bend (Figure 5d). The crystal structure of the nanowire at the position of the bend was examined by TEM to determine the mechanism involved in plastic deformation of the nanowires. Figure 5 shows TEM images of such bent nanowires. At the point of maximum compressive and tensile strain, the nanowire has become amorphous. This observation of amorphization prior to fracture is consistent with the layer of amorphous material that we also observed on fractured surfaces, as in Figure 2d.

At the onset of fracture, crack initiation appeared to occur in the amorphous region of the nanowire at the outer strained surface. Experimental and computational studies have shown a transition from crystalline to amorphous structure in strained Si nanowires through an increase in disorder brought about by a large increase in the population of dislocations.[13,32] Indentation studies of crystalline Ge have also shown sudden phase transformations to amorphous Ge (a-Ge) at high loads.[33] The authors of that study speculated that the transformation could occur by the formation of a high-pressure metallic phase followed by quenching to a-Ge as the pressure is released. Considering the large compressive stresses experienced in these specimens, both mechanisms are plausible. However, the detailed mechanism of the mechanically induced amorphization process requires further study.

The large quantity of Ge nanowires produced by the SFLS method and their high flexibility allows for the fabrication of a nonwoven ceramic fabric, or paper, of Ge nanowires. Figures 7 and 8 show photographs and SEM images of such Ge nanowire fabric fabricated by vacuum-filtration. The thickness of the fabric can be varied by changing the nanowire loading on the filter. For instance, 7.5 μm thick fabric (Figure 8a) required approximately 0.5 mg of nanowires, and 25 μm thick paper (Figure 8b) used approximately 1.25 mg. On the basis of the mass and dimensions of the nanowire paper, the density is approximately 10% of the density of bulk Ge, containing roughly 10% Ge nanowires and 90% void space by volume.

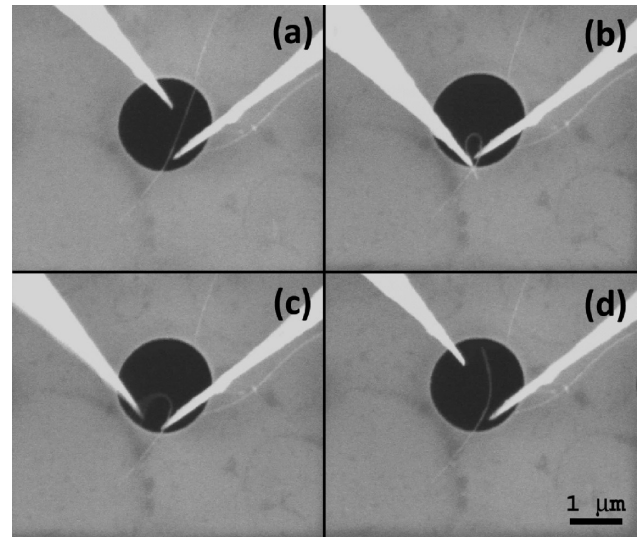

Figure 5. Sequence of SEM images of a Ge nanowire being manipulated with two tungsten nanomanipulator probes. From panels a to b the nanowire was cut with one of the probes and then bent to a high strain position. The probe has released the nanowire in panel c. Panel d shows the plastic deformation of the nanowire (see movie in Supporting Information).

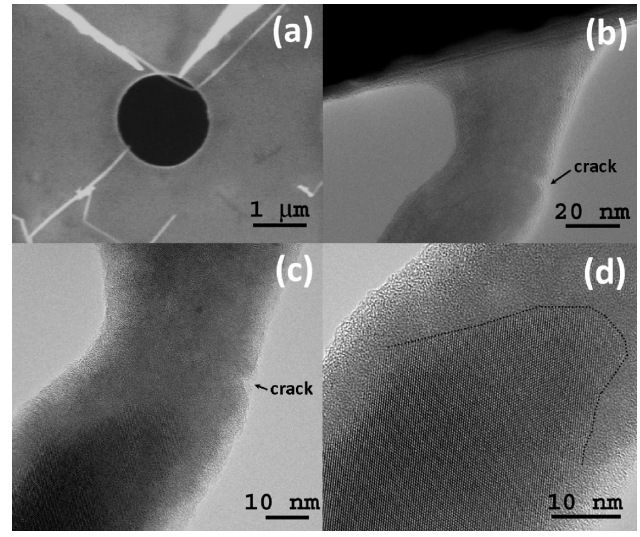

Figure 6. (a) SEM image of a cantilevered Ge nanowire bent to a high strain position and pinned to the SiN substrate by van der Waals forces. (b,c) HRTEM images of the region of highest strain area with the presence of crack formation. The delineation between the diamond-cubic and amorphous phases is clearly shown (dotted line) in HRTEM image d.

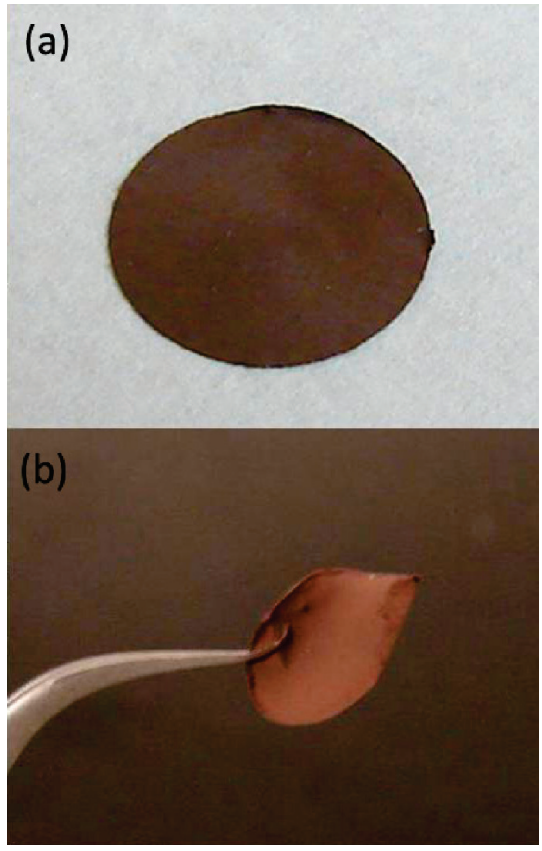

Figure 7. (a) Ge nanowire fabric drying on an alumina membrane filter. (b) Ge nanowire fabric after removal from the filter. The nanowire fabric is about 13 mm in diameter.

The bottom and top surfaces of the nanowire fabric had slightly different textures. As the SEM images in Figure 9 show, the side of the fabric that initially interfaces with the filter is much smoother than the top surface. On the top surface, there is the appearance of some nanowire bundling, which became more pronounced for thicker fabric samples. As the fabric becomes thicker, the filtering process slows considerably and nanowires become more susceptible to bundling and aggregation as they are pulled from the solvent onto the fabric surface. Most likely, this surface roughness could be reduced with nanowires with better dispersibility or by optimizing the vacuum pressure. Studies of the optical, electronic, and mechanical properties of this new class of material are currently underway.

CONCLUSIONS

The maximum radius of curvature and flexural strain of individual Ge nanowires with diameters between 23 and 97 nm were measured by bending with tungsten probes to the point of fracture. The Ge nanowires are extremely flexible, allowing bending down to a 67 nm radius of curvature for the smallest diameter. Ge nanowires were found to tolerate exceptionally high

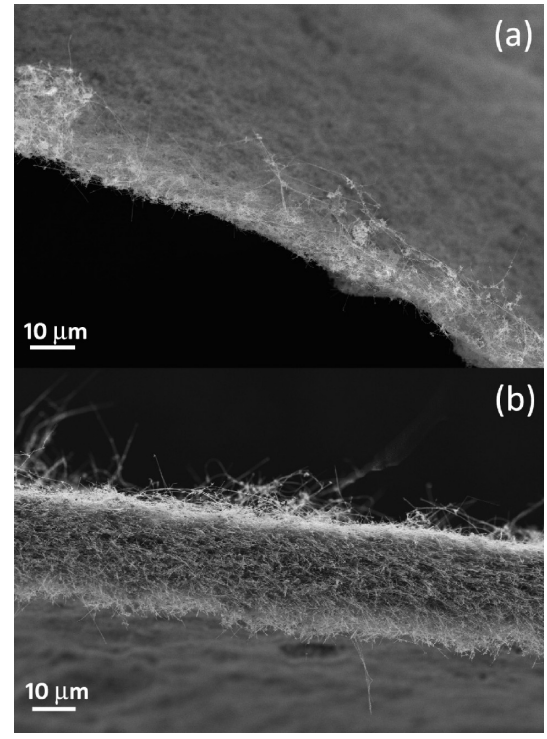

Figure 8. SEM images of the edges of (a) thin and (b) thick Ge nanowire fabric.

strains up to 17%, well in excess of the values of bulk Ge. The maximum radius of curvature and maximum strain increased with decreasing nanowire diameter, as expected from a decrease in defects in the reduced volume of the material. The bending strengths of Ge nanowires were determined and found to equal the

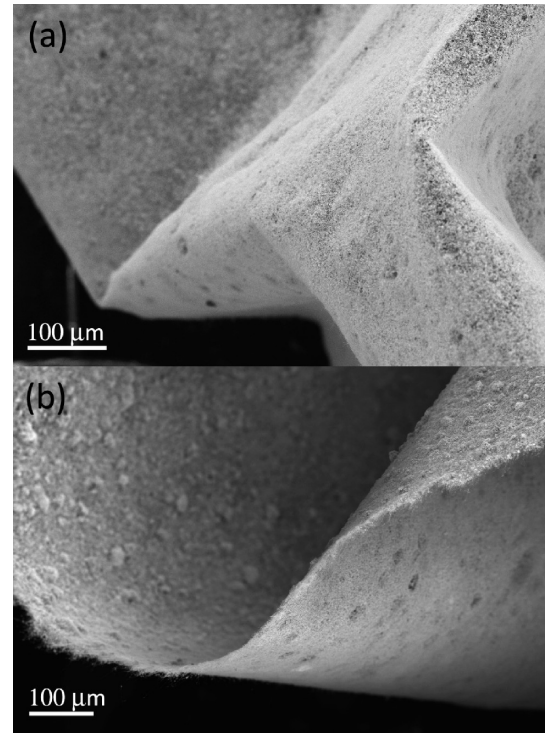

Figure 9. (a,b) SEM images of sections of Ge nanowire paper.

theoretical fracture strengths of a defect-free, perfect crystalline solid as their diameters were reduced. The corresponding strength-to-weight ratio of the Ge nanowires found in this study is as high as 33.8 kN m/kg, well above many commonly used fiber reinforcements (see Table 1). Room temperature plasticity was also observed at extremely high strains. Plastically deformed Ge nanowires exhibited amorphization at the point of maximum strain. In addition, the fabrication of a highly flexible ceramic fabric of Ge nanowires was demonstrated. This study demonstrates the remarkable flexibility and strength of Ge nanowires and illustrates their potential as building blocks for a variety of applications.

MATERIALS AND METHODS

Ge nanowires were synthesized by a gold nanocrystal-seeded SFLS process with surface passivation by exposure to isoprene using previously reported procedures.[7−9]

Single Nanowire Mechanical Measurements. Mechanical measurements were performed using a Zyvex S100 nanomanipulation system inside of a FEI Strata 235 dual beam SEM/FIB system. Tungsten probes were made by electrochemically etching tungsten wire (Goodfellow, 0.25 mm, 99.95% purity) in 2 M KOH at a bias of 4 V. The nanomanipulator was used to bend nanowires until fracture or to a high strain position. Video of specimen manipulation was obtained by splitting the monitor signal and capturing the split signal on a separate computer using a VGA2USB VGA capture device from Epiphan Systems Inc. The video was recorded at a frame rate faster than the SEM scan rate of 3 frames per second.

Fabrication of Nanowire Fabric. Ge nanowire fabric was made by vacuum-filtering a dilute dispersion of nanowires in chloroform (~0.1 mg/mL) through porous alumina filters (Whatman Anodisc 13, 0.2 μm pores). The fabric was then air-dried for 1 h and peeled from the filter.

Acknowledgment. This work was supported by the Robert A. Welch Foundation (F-1464), the Air Force Research Laboratory (FA-8650-07-2-5061), and the Office of Naval Research (N00014-05-1-0857). VCH acknowledges the Fannie and John Hertz Foundation and the NSF Graduate Research Fellowship Program for financial support.

Supporting Information Available: Movies of a Ge wire fractured by two tungsten nanomanipulator probes and a plastically deformed Ge nanowire. This material is available free of charge *via* the Internet at http://pubs.acs.org.

REFERENCES AND NOTES

1. Clarke, D. R. In *The Mechanical Properties of Semiconductors*; Faber, K. T., Malloy, K. J., Eds.; Academic Press, Inc.: San Diego, CA, 1992; Vol. 37.
2. Pearson, G. L.; Read, W. T.; Feldmann, W. L. Deformation and Fracture of Small Silicon Crystals. *Acta Metall.* **1957**, *5*, 181–191.
3. Barrett, C. R.; Nix, W. D.; Tetelman, A. S. *The Principles of Engineering Materials*; Prentice-Hall, Inc.: Englewood Cliffs, NJ, 1973.
4. Macmillan, N. H. The Theoretical Strength of Solids. *J. Mater. Sci.* **1972**, *7*, 239–254.
5. Claeys, C. *Germanium-Based Technologies: From Materials to Devices*; Elsevier Science: Oxford, 2007.
6. Davidson, F. M.; Lee, D. C.; Fanfair, D. D.; Korgel, B. A. Lamellar Twinning in Semiconductor Nanowires. *J. Phys. Chem. C* **2007**, *111*, 2929–2935.
7. Hanrath, T.; Korgel, B. A. Nucleation and Growth of Germanium Nanowires Seeded by Organic Monolayer-Coated Gold Nanocrystals. *J. Am. Chem. Soc.* **2002**, *124*, 1424–1429.
8. Hanrath, T.; Korgel, B. A. Supercritical Fluid−liquid−solid (SFLS) Synthesis of Si and Ge Nanowires Seeded by Colloidal Metal Nanocrystals. *Adv. Mater.* **2003**, *15*, 437–440.
9. Hanrath, T.; Korgel, B. A. Chemical Surface Passivation of Ge Nanowires. *J. Am. Chem. Soc.* **2004**, *126*, 15466–15472.
10. Ngo, L. T.; Almecija, D.; Sader, J. E.; Daly, B.; Petkov, N.; Holmes, J. D.; Erts, D.; Boland, J. J. Ultimate-Strength Germanium Nanowires. *Nano Lett.* **2006**, *6*, 2964–2968.
11. Hoffmann, S.; Utke, I.; Moser, B.; Michler, J.; Christiansen, S. H.; Schmidt, V.; Senz, S.; Werner, P.; Gosele, U.; Gallif, C. Measurement of the Bending Strength of Vapor−Liquid−Solid Grown Silicon Nanowires. *Nano Lett.* **2006**, *6*, 622–625.
12. Zheng, K.; Han, X.; Wang, L.; Zhang, Y.; Yue, Y.; Qin, Y.; Zhang, X.; Zhang, Z. Atomic Mechanisms Governing the Elastic Limit and the Incipient Plasticity of Bending Si Nanowires. *Nano Lett.* **2009**, *9*, 2471–2476.
13. Han, X.; Zheng, K.; Zhang, Y. F.; Zhang, X.; Zhang, Z.; Wang, Z. L. Low-Temperature *in Situ* Large-Strain Plasticity of Silicon Nanowires. *Adv. Mater.* **2007**, *19*, 2112–2118.
14. Xu, G. In *Dislocations in Solids*; Nabarro, F. R. N., Hirth, J. P., Eds.; North Holland: The Netherlands, 2004; Vol. 12, p 83.
15. Ruoff, R. S.; Qian, D.; Liu, W. K. Mechanical Properties of Carbon Nanotubes: Theoretical Predictions and Experimental Measurements. *C. R. Phys.* **2003**, *4*, 993–1008.
16. Smith, D. A.; Holmberg, V. C.; Lee, D. C.; Korgel, B. A. Young's Modulus and Size-Dependent Mechanical Quality Factor of Nanoelectromechanical Germanium Nanowire Resonators. *J. Phys. Chem. C* **2008**, *112*, 10725–10729.
17. Kumar, S.; Wang, Y. In *Composites Engineering Handbook*; Mallick, P. K., Ed.; Marcel Dekker, Inc.: New York, 1997.
18. Ruoff, R. S.; Lorents, D. C. Mechanical and Thermal Properties of Carbon Nanotubes. *Carbon* **1995**, *33*, 925–930.
19. Law, M.; Goldberger, J.; Yang, P. Semiconductor Nanowires and Nanotubes. *Annu. Rev. Mater. Res.* **2004**, *34*, 83–122.
20. Wong, E. W.; Sheehan, P. E.; Lieber, C. M. Nanobeam Mechanics: Elasticity, Strength, and Toughness of Nanorods and Nanotubes. *Science* **1997**, *277*, 1971–1975.
21. Lee, B.; Rudd, R. E. First-Principles Study of the Young's Modulus of Si ⟨001⟩ Nanowires. *Phys. Rev. B* **2007**, *75*, 041305−1–4.
22. He, R.; Yang, P. Giant Piezoresistance Effect in Silicon Nanowires. *Nature* **2006**, *1*, 42–46.
23. Park, S. H.; Cai, W.; Espinosa, H. D.; Huang, H. Mechanics of Crystalline Nanowires. *MRS Bull.* **2009**, *34*, 178–183.
24. Hsin, C. L.; Mai, W.; Gu, Y.; Gao, Y.; Huang, C. T.; Liu, Y.; Chen, L. J.; Wang, Z. L. Elastic Properties and Buckling of Silicon Nanowires. *Adv. Mater.* **2008**, *20*, 3919–3923.
25. Wu, B.; Heidelberg, A.; Boland, J. J. Mechanical Properties of Ultrahigh-Strength Gold Nanowires. *Nature* **2005**, *4*, 525–529.
26. Chen, X.; Zhang, S.; Wagner, G. J.; Ding, W.; Ruoff, R. S. Mechanical Resonance of Quartz Microfibers and Boundary Condition Effects. *J. Appl. Phys.* **2004**, *95*, 4823–4828.
27. Roesler, J.; Harders, H.; Baeker, M. *Mechanical Behaviour of Engineering Materials*; Springer: New York, 2007.
28. Roundy, D.; Cohen, M. L. Ideal Strength of Diamond, Si, and Ge. *Phys. Rev. B* **2001**, *64*, 212103-1–3.
29. Tabib-Azar, M.; Nassirou, M.; Wang, R. Mechanical Properties of Self-Welded Silicon Nanobridges. *Appl. Phys. Lett.* **2005**, *87*, 113102−1–3.
30. Gordon, M. J.; Baron, T.; Dhalluin, F.; Gentile, P.; Ferret, P. Size Effects in Mechanical Deformation and Fracture of Cantilevered Silicon Nanowires. *Nano Lett.* **2009**, *9*, 525–529.

31. Namazu, T.; Isono, Y.; Tanaka, T. Evaluation of Size Effect on Mechanical Properties of Single Crystal Silicon by Nanoscale Bending Test Using AFM. *J. Microelectromech. Syst.* **2000**, *9*, 450–459.
32. Menon, M.; Srivastava, D.; Ponomareva, I.; Chernozatonski, L. A. Nanomechanics of Silicon Nanowires. *Phys. Rev. B* **2004**, *70*, 125313-1–6.
33. Oliver, D. J.; Bradby, J. E.; Williams, J. S. Giant Pop-Ins and Amorphization in Germanium During Indentation. *J. Appl. Phys.* **2007**, *101*, 043524-1−9.